

The discovery of (*R*)-2-(*sec*-butylamino)-*N*-(2-methyl-5-(methylcarbamoyl)phenyl) thiazole-5-carboxamide (BMS-640994)—A potent and efficacious p38 α MAP kinase inhibitor

John Hynes, Jr.,* Hong Wu, Sidney Pitt, Ding Ren Shen, Rosemary Zhang, Gary L. Schieven, Kathleen M. Gillooly, David J. Shuster, Tracy L. Taylor, XiaoXia Yang, Kim W. McIntyre, Murray McKinnon, Hongjian Zhang, Punit H. Marathe, Arthur M. Doweyko, Kevin Kish, Susan E. Kiefer, John S. Sack, John A. Newitt, Joel C. Barrish, John Dodd and Katerina Leftheris

Bristol-Myers Squibb, Princeton, NJ 08543-4000, USA

Received 17 January 2008; revised 11 February 2008; accepted 13 February 2008

Available online 16 February 2008

Abstract—A novel structural class of p38 α MAP kinase inhibitors has been identified via iterative SAR studies of a focused deck screen hit. Optimization of the lead series generated **6e**, BMS-640994, a potent and selective p38 α inhibitor that is orally efficacious in rodent models of acute and chronic inflammation.

© 2008 Elsevier Ltd. All rights reserved.

The protein-based pharmacological blockade of pro-inflammatory signaling molecules, specifically TNF- α is emerging as an important therapeutic option for the treatment of rheumatoid arthritis (RA) and other inflammatory diseases.^{1,2} Upon activation, p38 mitogen-activated protein kinase (MAPK), a serine-threonine kinase consisting of 4 isoforms, up-regulates the biosynthesis of two pro-inflammatory cytokines, TNF α and IL-1 β .³ Accordingly, modulation of the p38 signaling cascade has emerged as an attractive target for the design of novel chemotherapeutic agents for the treatment of inflammatory diseases.^{4–6} Expression of the p38 MAPK isoforms varies across cell types of the immune system and it is believed that the predominant isoform involved in inflammation is p38 α .⁷

We have previously reported the in vitro and in vivo evaluation of pyrrolo[2,1-*f*][1,2,4]triazine-based p38 α inhibitors (**1**, Fig. 1).⁸ In this letter, we report the discov-

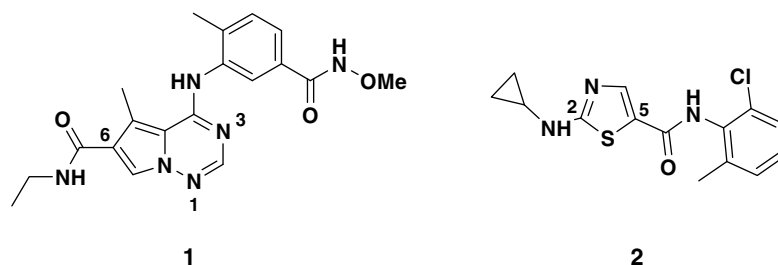
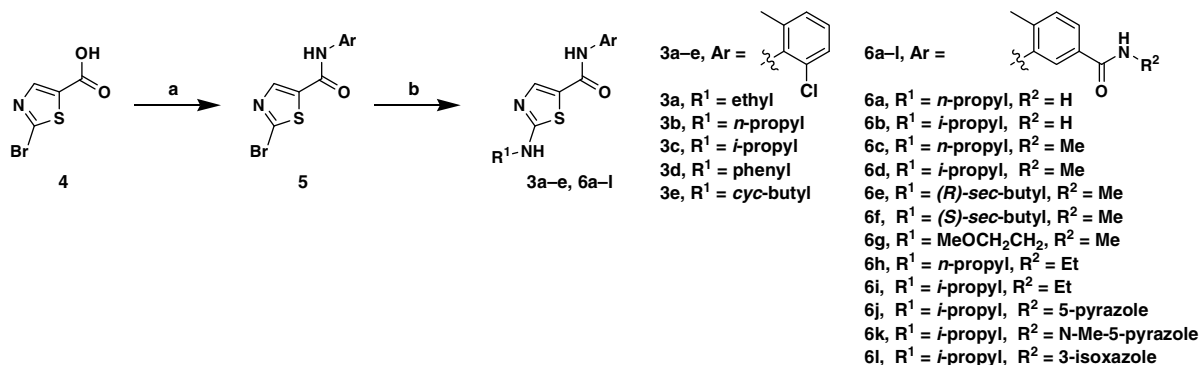
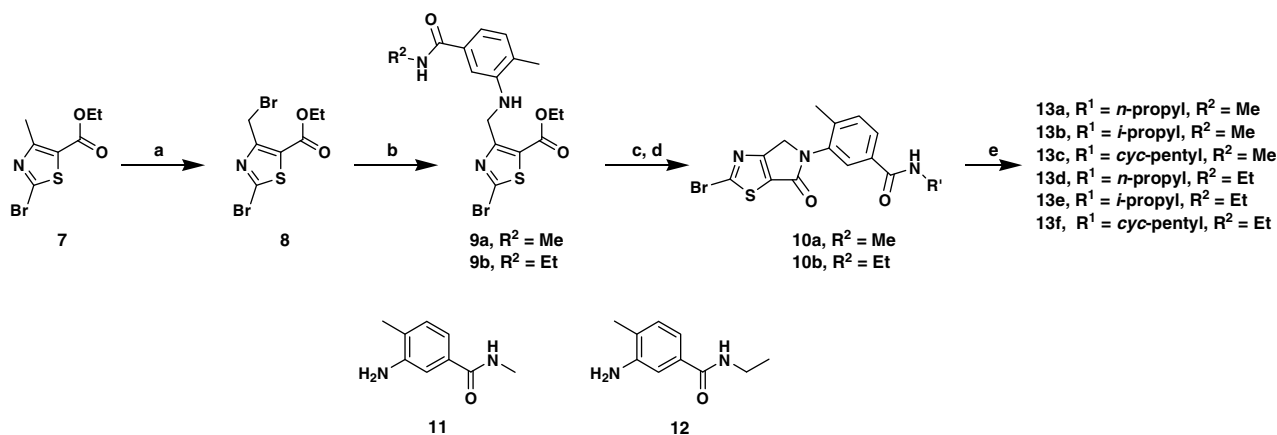
ery, in vitro SAR, and in vivo efficacy of 2-alkylamino-5-carboxamidoaniline thiazole-derived p38 α inhibitors.

A focused screen of internal kinase inhibitors identified C2-alkylaminothiazole **2** (Fig. 1) as a moderately potent p38 α kinase inhibitor (IC₅₀ 39 ± 10 nM) with limited potency in a cell-based functional assay measuring TNF α biosynthesis (human PBMC IC₅₀ ~ 1.5 μ M).⁹ This compound was originally derived from a program directed towards identifying inhibitors of the tyrosine kinase p56^{Lck} (Lck IC₅₀ 140 nM for **2**).¹⁰ We envisioned that the structural diversity of this series relative to the previously studied pyrrolo[2,1-*f*][1,2,4]triazines would produce divergent in vitro and in vivo profiles. Subsequently, we undertook an SAR effort aimed at increasing p38 α inhibition, cellular potency, and kinase selectivity, with the goal of producing efficacious compounds in multiple in vivo models of inflammation.

The compounds were synthesized according to the procedures outlined in Schemes 1 and 2. Briefly, 2-bromothiazole-5-carboxylic acid (**4**) was coupled to a variety of aryl amines to afford **5**. Nucleophilic displacement of the C2 halogen with various amines was accomplished at

Keywords: p38; MAP kinase; Aminothiazole; TNF.

* Corresponding author. Tel.: +1 609 252 4431; fax: +1 609 252 3993; e-mail: john.hynes@bms.com

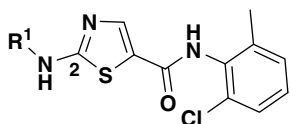
Figure 1. BMS p38 α inhibitors.Scheme 1. Reagents and conditions: (a) Ar–NH₂, EDC, HOBt, DIPEA, DMF, rt; (b) R¹–NH₂, EtOH, 150 °C.Scheme 2. Reagents and conditions: (a) NBS, AIBN, CCl₄, Δ, 54%; (b) **11** or **12**, K₂CO₃, DMF, rt, 80–83%; (c) 1 N NaOH, THF, MeOH, 70–87%; (d) EDC, CH₂Cl₂, 0 °C, 91–98%; (e) R¹–NH₂, EtOH, 150 °C, 50–80%.

high temperature to afford analogs **3a–e** and **6a–l**. The fused bicyclic aminothiazoles (**13a–f**) were prepared via the bromination of thiazole **7** to give **8**. Dibromide **8** was reacted with **11** or **12** to give **9a** or **9b**. Hydrolysis of the ester was followed by EDC-mediated lactam formation to afford the intermediate bromides **10a** and **10b**. These were reacted with a variety of amines to provide analogs **13a–f**.

The synthesized C2-aminothiazole analogs were screened and optimized for inhibition of human p38 α MAP kinase. Compounds with significant enzyme inhibition (IC₅₀ < 50 nM) were then evaluated in a human lipopolysaccharide (LPS)-induced TNF α biosynthesis assay in human peripheral blood mononuclear cells (PBMCs).

Table 1 summarizes the in vitro potency of the C2 amino variants of **2**. Branched acyclic and cyclic C2 substitution was well tolerated in the p38 α enzyme inhibition assay. The aryl amine **3d** had reduced enzyme inhibition relative to **2**, as did the C2 ethylamine analog **3a**. In the PBMC functional assay, **3c** was potent, whereas **3b** was inactive in this assay.

The inability to significantly enhance p38 α and TNF α inhibition via C2 modification, combined with the lack of Lck selectivity (i.e., **3e**), prompted us to modify our compound design strategy. Based upon our previous studies,⁸ we hypothesized that the replacement of the aniline of **2** with the *meta*-substituted carboxamide anilines found in **1** would enhance p38 α kinase inhibition, cellular potency, and selectivity for p38 α against Lck.

Table 1. Preliminary C2 SAR

Compound	R ¹	IC ₅₀ (nM)		
		p38α ^a	TNFα ^b	Lck ^c
2	<i>cyc</i> -Propyl	39	1500	140
3a	Ethyl	140	nt ^d	
3b	<i>n</i> -Propyl	28	>2000	
3c	<i>i</i> -Propyl	13	160	
3d	Phenyl	62	nt ^d	
3e	<i>cyc</i> -Butyl	36	nt ^d	3310

^a Compounds were assayed in triplicate. Variability around the mean value was <50%.

^b Compounds were typically assayed in duplicate.

^c *n* = 1.

^d nt, not tested.

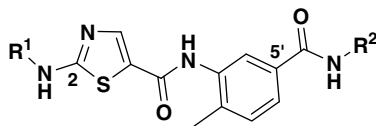
As shown in Table 2, >3-fold increases in p38α enzyme and human PBMC potency were observed when 2-methyl-5-carboxamide anilines were substituted in the place of 2-chloro-6-methyl aniline. A trend towards an increased cellular potency was observed when the C2 substituent contained a branched aliphatic group (e.g., **6c** vs **6e** and **6f**). Ether incorporation within the C2 chain (**6g**) decreased enzyme and cellular potency. C5' heterocyclic amides (**6j–l**) were tolerated in both assays.

In general, selectivity against Lck (>1000-fold) was observed, with the exception of the amino-isoxazole **6l** (Lck IC₅₀ 380 nM).

The conformationally restricted fused lactams (**13a–f**) had decreased p38α inhibition relative to the C4 unsubstituted analogs and, when tested, were weak inhibitors in the PBMC functional assay (Table 3). C4 methyl substituted analogs (**14a,b**, Table 3) had decreased p38α enzyme inhibition and were not pursued further.

Advanced compounds were evaluated in a murine model of acute inflammation (mouse LPS-TNFα). Criteria for evaluation in this model included potent cell inhibition of LPS-induced TNFα (IC₅₀ < 15 nM) and reasonable Caco-2 permeability (>75 nm/s).¹¹ Several of the C5' methyl and ethyl amides met the above criteria and progressed into this model. Compounds were initially screened at 5 mg/kg dosed orally, using a 4 h pre-dosing interval to LPS challenge. A secondary screen using a 24 h pre-dosing interval was used to identify long-acting potent inhibitors (Table 4). Compound **6e** was efficacious in the 24 h pre-dosing protocol in mice and progressed into a dose–response study in rats, whereby an oral ED₅₀ of 2 mg/kg was obtained (Fig. 2).

Compound **6e** was then subjected to advanced in vitro pharmacological and profiling assays, some of which are highlighted in Table 5. In addition to TNFα blockade, **6e** inhibited LPS-induced IL-1β production in

Table 2. Effect of the C2 and C5'-substituents on enzymatic and cellular activity

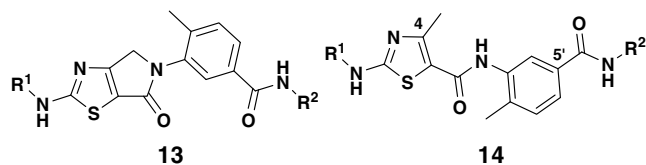
Compound	R ¹	R ²	IC ₅₀ (nM)		
			p38α ^a	TNFα ^b	Lck ^c
6a	<i>n</i> -Propyl	H	4.1	23	nt ^d
6b	<i>i</i> -Propyl	H	3.2	35	>50,000
6c	<i>n</i> -Propyl	Me	4.5	42	4800
6d	<i>i</i> -Propyl	Me	3.5	8.7	>50,000
6e	(<i>R</i>)- <i>sec</i> -butyl	Me	3.5	2.9	22,000
6f	(<i>S</i>)- <i>sec</i> -butyl	Me	2.3	4.1	>50,000
6g	MeOCH ₂ CH ₂	Me	22	>250	
6h	<i>n</i> -Propyl	Et	2.0	2.7	1900
6i	<i>i</i> -Propyl	Et	3.4	11	>50,000
6j	<i>i</i> -Propyl		4.2	7.9	nt ^d
6k	<i>i</i> -Propyl		5.4	6.4	5800
6l	<i>i</i> -Propyl		3.8	1.0	380

^a Compounds were assayed in triplicate. Assay variability was measured using a standard control, <40% (*n* = 46).

^b Compounds were typically assayed in duplicate. Assay variability was measured using a standard control, <80% (*n* = 25).

^c *n* = 1.

^d nt = not tested.

Table 3. C4 substituent SAR and fused ring thiazoles


Compound	R ¹	R ²	IC ₅₀ (nM)	
			p38α ^a	TNFα ^b
13a	<i>n</i> -Propyl	Me	270	
13b	<i>i</i> -Propyl	Me	110	
13c	<i>cyc</i> -Pentyl	Me	110	
13d	<i>n</i> -Propyl	Et	160	
13e	<i>i</i> -Propyl	Et	34	>250
13f	<i>cyc</i> -Pentyl	Et	53	240
14a	Ethyl	Et	330	
14b	<i>n</i> -Propyl	Et	130	

^a Compounds were assayed in triplicate. Assay variability was measured using a standard control, <40% ($n = 46$).

^b Compounds were typically assayed in duplicate. Assay variability was measured using a standard control, <80% ($n = 25$).

Table 4. Inhibition of circulating TNFα in LPS-challenged mice dosed orally with 5 mg/kg of compound

Entry	Compound	Dosing interval (h)	% Inhib ^a	Drug serum Conc. (nM)
1	6d	-4 ^b	62 ± 11 ^c	400 ± 190
2	6f	-4 ^b	69 ± 8.9 ^c	250 ± 46
3	6i	-4 ^b	68 ± 13 ^c	330 ± 110
4	6h	-24	na ^d	Not measured
5	6e	-24	46 ± 31 ^c	Not measured

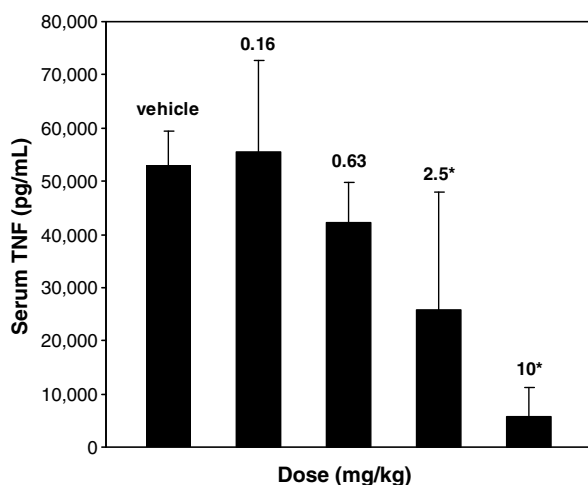
^a Percent reduction in circulating TNFα, mean ± SD, $n = 8$ animals.

^b Not active at 24 h pre-dosing interval.

^c $p < 0.001$ versus vehicle, Student's *T*-test.

^d na, not active.

^e $p < 0.05$ versus vehicle, Student's *T*-test.

**Figure 2.** Inhibition of LPS-induced TNFα in rats by compound 6e.¹²

PBMCs (IC₅₀ 99 nM). Furthermore, in human whole blood, LPS-induced TNFα and IL-1β were inhibited with IC₅₀ values of 54 and 600 nM, respectively. Across

Table 5. In vitro profiling data for compound 6e

Parameter	Result
LPS-IL-1β IC ₅₀	99 ± 36 nM
WB LPS-TNFα IC ₅₀	54 ± 44 nM
WBLPS-IL-1β IC ₅₀	600 ± 397 nM
Metabolism ^a	HLM, RLM, MLM 0.00 ^b
CYP inhibition ^c	>40 μM 1A2, 2C9, 2C19, 2D6, 3A4
hERG ^d	7% inhib at 30 μM
Kinases (~64)	>1000-fold selective
p38β, γ, δ IC ₅₀ (nM)	1.5, > 30,000, > 30,000
Protein binding	Human-82%; Rat-89%
Caco-2 permeability	83 nm/s
Aq. sol., pH 6.5	0.022 mg/mL

^a HLM, human liver microsomes; RLM, rat liver microsomes; MLM, mouse liver microsomes.

^b nmol/min/mg.

^c CYP, cytochrome P450.

^d Patch clamp assay.

multiple species, **6e** had minimal liver microsomal turnover. Minimal hERG channel or Cyp isoform inhibition was observed. When screened against a panel of kinases, **6e** was shown to be highly selective for p38α. Among the four p38 isoforms, only p38α and p38β were potently inhibited (IC₅₀ 1.5 nM). The physicochemical properties of **6e** (protein binding, Caco-2 permeability, and aqueous solubility) are also summarized.

When dosed in rats, compound **6e** was orally bioavailable (%*F* = 75), had moderate clearance, and a reasonable half-life (Table 6). High levels of serum drug levels were obtained (*C*_{max} and AUC_{0–24h}) through the course of the study.

Table 6. Pharmacokinetic properties of 6e in rats

Parameter	Value ^a
iv dose (1 mg/kg)	
<i>t</i> _{1/2} (h)	1.8
CL (mL/min/kg)	14.1
<i>V</i> _{ss} (L/kg)	1.8
po dose (10 mg/kg)	
<i>C</i> _{max} (μM)	8.7 ± 2.2
AUC _{0–24h} (μM-h)	25 ± 2.3
<i>C</i> _{24h} (nM)	7.6 ± 3.5
% <i>F</i>	75

^a Vehicle: PEG300. $n = 3$ animals.

The favorable acute efficacy in rodents, in vitro profiling data, and aforementioned PK properties supported the advancement of **6e** into the advanced disease models of chronic inflammation. In the rat adjuvant-induced arthritis model, **6e** significantly inhibited disease progression at 1 and 3 mg/kg, (po, qd) as measured by paw swelling (Fig. 3). A minimally efficacious dose of 0.3 mg/kg, (po, qd) for **6e** was obtained (46% inhibition, data not shown). Micro computed tomography (CT) imaging of isolated rat hocks revealed that drug-treated animals (0.3 mg/kg, po, qd) had minimal disease progression or bone degeneration.¹³

Compound **6e** was co-crystallized with p38α MAP kinase and the structure of the complex was determined via X-ray diffraction (Fig. 4). Consistent with previous

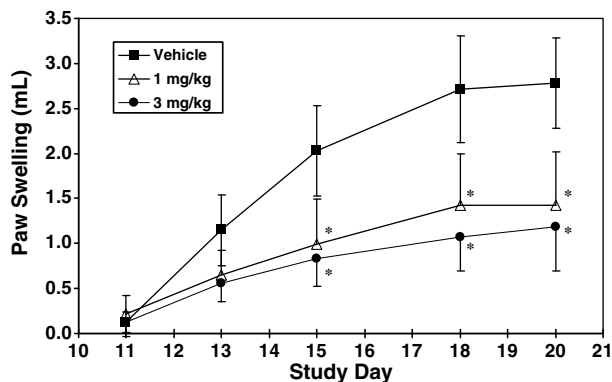


Figure 3. Efficacy of Compound **6e** in the Rat Adjuvant Arthritis Model (qd, po). Terminal serum concentrations (18 h after final dose) for **6e** at 1 and 3 mg/kg were 8.1 and 16 nM, respectively.

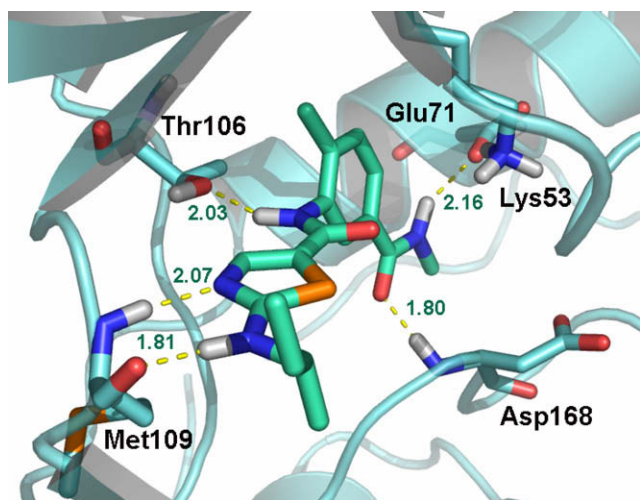


Figure 4. X-ray structure of **6e** co-crystallized with p38 α .¹⁶

p38 α inhibitors containing a *meta*-substituted carboxamide aniline, the C5' carboxamide NH and CO form hydrogen bonds with Glu71 (2.1 Å) and Asp168 (1.8 Å), respectively. The thiazole ring nitrogen forms a hydrogen bond (2.0 Å) with the backbone NH of Met109. An additional hydrogen bond interaction is gained between the Met109 carbonyl and the C2 amine NH (1.8 Å).¹⁴ The observed deleterious effects of C4 substitution (i.e., compounds **13–14**) can be rationalized from this structure due to the projection of the C4 substituent towards the His107–Thr106 region surface and disruption of a Thr106 hydrogen bond interaction with the pendant C5 amide NH. Examination of recently published Lck X-ray structures reveals a significant difference in the conformation of the inner region of the activation loop (168–172 in p38 corresponding to 382–386 in Lck).¹⁵ In the case of p38, the C5' benzamide carbonyl oxygen can engage in a H-bond to the backbone NH at Asp168, while the trajectory of Glu71 is aimed away from this region. In the case of Lck, the corresponding Glu (Glu288) appears to be H-bonding to the backbone NH at Phe383 (Phe169 in p38), which may block a benzamide approach to the adjacent NH (at Asp168).

In summary, a novel series of potent and selective C2-alkylaminothiazole p38 α MAP kinase inhibitors has been identified. Structure–activity studies led to the discovery of (*R*)-2-(*sec*-butylamino)-*N*-(2-methyl-5-(methylcarbamoyl)phenyl) thiazole-5-carboxamide **6e** (BMS-640994), which was orally efficacious in acute and chronic models of inflammation. The molecular basis for p38 α kinase interactions for this class of inhibitors has been established via X-ray crystallography.

Acknowledgment

The authors thank Georgia Cornelius of the Department of Bioanalytical Research for obtaining serum concentrations for the in vivo studies.

References and notes

- (a) Choy, E. H. S.; Panayi, G. S. *N. Eng. J. Med.* **2001**, *344*, 907; (b) Dinarello, C. A. *Curr. Opin. Immunol.* **1991**, *3*, 941.
- (a) Palladino, M. A.; Bahjat, F. R.; Theodorakis, E. A.; Moldawer, L. L. *Nat. Rev. Drug Disc.* **2003**, *2*, 736; (b) Braddock, M.; Quinn, A. *Nat. Rev. Drug Disc.* **2004**, *3*, 1.
- (a) Salituro, F. G.; Germann, U. A.; Wilson, K. P.; Bemis, G. W.; Fox, T.; Su, M. S. *Curr. Med. Chem.* **1999**, *6*, 807; (b) Foster, M. L.; Halley, F.; Souness, J. E. *Drug News Perspect.* **2000**, *13*, 488; (c) Kumar, S.; Boehm, J.; Lee, J. C. *Nat. Rev. Drug Disc.* **2003**, *2*, 717; (d) Saklatvala, J. *Curr. Opin. Pharmacol.* **2004**, *4*, 372; (e) Kumar, S.; Blake, S. M. *Handb. Exp. Pharmacol.* **2005**, *167*, 65.
- Westra, J.; Limburg, P. C. *Mini-Rev. Med. Chem.* **2006**, *6*, 867.
- For reviews detailing the current small molecule p38 kinase inhibitor field see: (a) Hynes, J.; Leftheris, K. *Curr. Top. Med. Chem.* **2005**, *5*, 967; (b) Wagner, G.; Laufer, S. *Med. Res. Rev.* **2006**, *1*, 1; (c) Lee, M. R.; Dominguez, C. *Curr. Med. Chem.* **2005**, *12*, 2979.
- (a) Fijen, J. W.; Zijlstra, J. G.; De Boer, P.; Spanjersberg, R.; Cohen Tervaert, J. W.; van der Werf, T. S.; Lightenberg, J. J. M.; Tulleken, J. E. *Clin. Exp. Immunol.* **2001**, *124*, 16; (b) Branger, J.; van den Blink, B.; Weijer, S.; Madwed, J.; Bos, C. L.; Gupta, A.; Yong, C.-L.; Polmar, S. H.; Olszyna, D. P.; Hack, E. C.; van Deventer, S. J. H.; Peppelenbosch, M. P.; van der Poll, T. *J. Immunol.* **2002**, *168*, 4070.
- (a) Hale, K. K.; Trollinger, D.; Rihaneck, M.; Manthey, C. L. *J. Immunol.* **1999**, *162*, 4246; (b) Allen, M.; Svensson, L.; Roach, M.; Hambor, J.; McNeish, J.; Gabel, C. A. *J. Exp. Med.* **2000**, *191*, 859; (c) Fearn, C.; Kline, L.; Gram, H.; Di Padova, F.; Zurini, M.; Han, J.; Ulevitch, R. *J. Leukocyte Biol.* **2000**, *67*, 705.
- Hynes, J., Jr.; Dyckman, A.; Lin, S.; Wroblewski, S. T.; Wu, H.; Gillooly, K. M.; Kanner, S. B.; Lonial, H.; Loo, D.; McIntyre, K. W.; Pitt, S.; Shen, D. R.; Shuster, D. J.; Yang, X.; Zhang, R.; Behnia, K.; Zhang, H.; Marathe, P. H.; Doweyko, A.; Tokarski, J. S.; Sack, J. S.; Pokross, M.; Kiefer, S. E.; Newitt, J. A.; Barrish, J. C.; Dodd, J.; Schieven, G. L.; Leftheris, K. *J. Med. Chem.* **2008**, *51*, 4.
- Peripheral blood mononuclear cells (PBMCs) are purified from human whole blood by Ficoll–Hypaque density gradient centrifugation and resuspended at a concentration of 5×10^6 /mL in assay medium (RPMI medium containing 10% fetal bovine serum). 50 μ L of cell suspension is incubated with 50 μ L of test compound (4 \times

- concentration in assay medium containing 0.2% DMSO) in 96-well tissue culture plates for 5 min at RT. 100 μ L of LPS (200 ng/mL stock) is then added to the cell suspension and the plate is incubated for 6 h at 37 °C. Following incubation, the culture medium is collected and stored at –20 °C. TNF α concentration in the medium is quantified using a standard ELISA kit (Pharmingen-San Diego, CA). Concentrations of TNF α and IC₅₀ values for test compounds (concentration of compound that inhibited LPS-stimulated TNF α production by 50%) are calculated by linear regression analysis.
10. Wityak, J.; Das, J.; Moquin, R. V.; Shen, Z.; Lin, J.; Chen, P.; Doweiko, A. M.; Pitt, S.; Pang, S.; Shen, D. R.; Fang, Q.; de Fex, H. F.; Schieven, G. L.; Kanner, S. B.; Barrish, J. C. *Bioorg. Med. Chem. Lett.* **2003**, *13*, 4007.
 11. The primary amides **6a** and **6b** had poor in vitro permeability and were not evaluated further.
 12. Male Lewis rats (Harlan labs, $n = 5$ /group) were dosed orally with compound solubilized in PEG300. Two hours after dosing, LPS (10 μ g, *Escherichia coli* O11:B4 strain from Sigma) was suspended in PBS (1 mL) and dosed IP. Ninety minutes after LPS challenge, the rats were bled and serum TNF α determined by Elisa (R&D Systems), according to the manufacturer's instructions. $p < 0.05$ versus vehicle, Student's *T*-test. Three out of 5 rats at the 10 mg/kg dose had undetectable levels of serum TNF α .
 13. Krishnan, B.; Kukral, D., Bristol-Myers Squibb, unpublished results.
 14. Fitzgerald, C. E.; Patel, S. B.; Becker, J. W.; Cameron, P. M.; Zaller, D.; Pikounis, V. B.; O'Keefe, S. J.; Scapin, G. N. *Nat. Struct. Biol.* **2003**, *10*, 764.
 15. (a) Martin, M. W.; Newcomb, J.; Nunes, J. J.; McGowan, D. C.; Armistead, D. M.; Boucher, C.; Buchanan, J. L.; Buckner, W.; Chai, L.; Elbaum, D.; Epstein, L. F.; Faust, T.; Flynn, S.; Gallant, P.; Gore, A.; Gu, Y.; Hseih, F.; Huang, X.; Lee, J. H.; Metz, D.; Middleton, S.; Mohn, D.; Morgenstern, K.; Morrison, M. J.; Novak, P. M.; Oliveira-dos-Santos, A.; Powers, D.; Rose, P.; Schneider, S.; Sell, S.; Tudor, Y.; Turci, S. M.; Welcher, A. A.; White, R. D.; Zack, D.; Zhao, H.; Zhu, L.; Ghiron, C.; Amouzegh, P.; Ermann, M.; Jenkins, J.; Johnston, D.; Napier, S.; Power, E. *J. Med. Chem.* **2006**, *49*, 4981; (b) Martin, M. W.; Newcomb, J.; Nunes, J. J.; Bemis, J. E.; McGowan, D. C.; White, R. D.; Buchanan, J. L.; DiMauro, E. F.; Boucher, C.; Faust, T.; Hseih, F.; Huang, X.; Lee, J. H.; Schneider, S.; Turci, S. M.; Zhu, Z. *Bioorg. Med. Chem. Lett.* **2007**, *17*, 2299.
 16. For details of the X-ray collection method, see Ref. 8. The coordinates for the structure in Figure 4 have been deposited with the RCSB Protein Data Bank, PDB ID code 3BX5.